Hindawi
Wireless Communications and Mobile Computing
Volume 2022, Article ID 2523196, 14 pages
https://doi.org/10.1155/2022/2523196

Research Article

Sea Experimental for Compressive Sensing-Based Sparse Channel Estimation of Underwater Acoustic TDS-OFDM System

Naveed Ur Rehman Junejo,[1,2] **Hamada Esmaiel**,[1,3] **Mariyam Sattar**,[4] **Haixin Sun**,[1] **Muhammad Amir Khalil**,[2] **and Ihsan Ullah**[2]

[1]*Department of Information and Communication, School of Informatics, Xiamen University, Xiamen 316005, China*
[2]*Deparment of Computer Engineering, The University of Lahore, 1-KM Defence Road, Lahore, Pakistan*
[3]*Electrical Engineering Department, Faculty of Engineering, Aswan University, Aswan 81542, Egypt*
[4]*Department of Mechanical Engineering, Institute of Space Technology, Islamabad, Pakistan*

Correspondence should be addressed to Hamada Esmaiel; h.esmaiel@aswu.edu.eg

Received 20 January 2022; Revised 24 March 2022; Accepted 7 April 2022; Published 5 May 2022

Academic Editor: Miaowen Wen

Due to the high spectral efficiency (SE) and fast synchronization, the time-domain synchronization orthogonal frequency division multiplexing (TDS-OFDM) system has gotten much more attraction of researchers as compared to cyclic-prefix (CP) and zero padding (ZP) OFDM in terrestrial as well as underwater acoustic communication. Inter-block interference (IBI) degrades the TDS-OFDM performance due to its long-delay multiple channels. In TDS-OFDM, dual pseudo-random noise (DPN) sequences utilize two PN sequences as a guard interval (GI) after every data block to cope with interference from the OFDM data block to the next PN sequence resulting in compromising the energy efficiency (EE) and spectral efficiency. We have proposed compressed sensing-based technique compressive sensing matching pursuit (CoSaMP), orthogonal matching pursuit (OMP), and look-ahead and backtracking OMP (LABOMP) for TDS-OFDM over the real-time underwater channel in this paper. Moreover, prior to estimating the channel, the received PN sequence is considered in the time domain to compensate for the Doppler shift of the UWA channel. The real-time data experiment has been initially conducted for testing in a water tank in our laboratory. Furthermore, it has been tested on the sea for long communications under the water at the Wuyuan sea area in Xiamen, China. Simulations and experimental results evident that the compressed sensing techniques have better performance over the conventional TDS-OFDM and DPN-TDS-OFDM, even LABOMP outperform OMP and CoSaMP in terms of bit-error-rate (BER), SE, and EE.

1. Introduction

The water has covered the major area of Earth's surface; nearly 71% of the earth is water covered. Such water is split into various principles such as small-scale seas, oceans, and rivers. Ocean tenderness commands the wind originals and the environment changes that make different lifestyles on top of the earth's surface. Lakes and rivers include no more than 1% of freshwater over the earth's surface. Its disease seriously harms ecosystems. The internet of underwater thighs (IoUT), the control of enormous areas of uncharted water [1]. The purpose of this study proposal is to propose a green underwater multicarrier modulation technique.

The full design supporting the accepted data rate with reliable communication IoUT nodes has been considered among one of the most challenging underwater communication problems due to the weak spread of electromagnetic waves in the water and the low data rate future in the case of acoustic waves propagation [2]. Recently, magnetic induction was proposed for underground and underwater data transmission, but unfortunately, ocean conductivity makes harsh attenuation for both the magnetic induction and electromagnetic signals. To prevail over that kind of attenuation problem, ultra-low frequency bands with very low data transmission rates should be used. With a high potential data rate, optical data transmission has been proposed for

underwater data transmission. Unfortunately, optical-based underwater communication systems suffer from modeling the chemical and physical traits of the water. Due to all the above, the acoustic-based underwater communication system is considered the broadest technology [3]. Research on underwater communication was mainly focused on increasing data rate over the limited acoustic bandwidth and solving acoustic-based problems such as high ambient noise, Doppler shift, and propagation delay [4].

The designing acoustic-based communication system should consider the natural features of the ocean media. Such features such as high attenuation power and such attenuation restrict and limit the communication distance. Plus, the transmitter and receiver motion due to water waves increase the Doppler Effect. Also, due to the variations in geography, underwater communication considers environmental-based communication and provides a non-uniformly fluctuated acoustic propagation [5]. To obtain reliable acoustic-based underwater communication researchers and industry go-to multicarrier modulation. Thanks to the multicarrier modulation, the data rate can be increased even over limited channel bandwidth such as acoustic-based underwater channels. Also mitigates the Doppler shift and unwanted inter symbol interference (ISI). Another advantage point of the multicarrier modulation technique is the easy equalization [6, 7]. The multicarrier technique is a reserve to defeat the long-time interval which creates a greater symbol period but shrinks the ISI. Due to all the above, the channel estimation technique can be a key parameter in providing reliable underwater and deserved great attention [8–10].

The multicarrier communication technique, i.e., orthogonal frequency division multiplexing (OFDM), is considered among the key notable underwater multicarrier modulation techniques. The OFDM technique is further divided into three main categories including (1) zero padding (ZP - OFDM), (2) cyclic-prefix (CP - OFDM), and (3) time-domain synchronization (TDS - OFDM) [11–13]. The difference between the three schemes is the inter-block interference (IBI) mitigation way over the multipath channels [11, 12]. Each way has its advantage and disadvantages. CP provides linear convolution and can be used for channel estimation at the expense of transmitted power. Unfortunately, saving the IoUT node's power is a very important point due to the hard recharging capability. ZP-OFDM solves the channel null problem and saves the transmitted power at the expense of the on-off problem [14]. TDS-OFDM technique, at the cost of the bit-error rate (BER) in the functioning of the system, presents exceptional power and energy efficiency [11, 15, 16]. In the present era, the system data rate has been increased following the technique of index modulation [17–20]. Unfortunately, the index modulation technique cannot support the long underwater communication distance as the multipath nature of the acoustic underwater channel can destroy the indexed data plus data recovery needs high receiver complexity.

In the multicarrier modulation, the guard interval technique is required to circumvent the inter-carrier interference (ICI) in the underwater acoustic channel, such long guard interval wastes the channel utilization. Such spectral loss will be more severe as the long tap delay underwater channel needs long pilots' signals. The overhead information of pilot's and guard interval waste IoUTs nodes as well as spectral. Energy saving is very important for a new modern communication system, and such importance is very effective in the IoUT nodes as the recharging capability is hard in the underwater communication and saving energy increases the battery lifetime. Therefore, based on that, the TDS-OFDM schemes and the ZP-OFDM systems are the utmost desired multicarrier modulation techniques. However, the energy-saving capability and the spectral efficiency of the ZP-OFDM system are low in comparison to the TDS-OFDM scheme. The primary disadvantage of the TDS-OFDM systems is the excessive BER owing to the IBI amid the OFDM data blocks and the pseudo-noise (PN) sequences introduced in the guard intervals. The researchers focused on reducing and removing such IBI with different methods such as interference cancelation based on the iterative algorithm [21], and with addition without fluctuations in the frame construction of the TDS-OFDM scheme [22]. Unfortunately, these schemes slightly improve the TDS-OFDM BER performance [23], and such schemes cannot support a reliable TDS-OFDM-based underwater acoustic communication. Different BER improvement methods of the TDS-OFDM are changing the frame structure, and the modified frame structure is based on interference cancelation [23]. In the proposed unique word (UW) OFDM system, the time domain guard interval is produced by assigning the redundant pilots in the frequency domain [24]. Unfortunately, the UW-OFDM complexity is high without interference-free for the OFDM data blocks. Dual PN sequences have been used for TDS-OFDM in [23, 25, 26] to receive OFDM without inference. Dual PN simplified the channel estimation and equalization, but duplicate guard interval reduces the spectral efficiency. Duplication for guard interval is inapplicable for IoUT, as a duplicate of the guard interval is a waste of energy and spectrum.

Owing to the reduced length of multipath intervals than the channel spread, the channel impulse response (CIR) is sparse in the channel of underwater acoustics [27]. Therefore, the compressive sensing theory is applied for sparse channel estimation because of the sparse performance of the underwater channel [3, 28–30]. This paper applies the methods of CS theory to estimate the underwater CIR by using a small region free from the IBI. This arrangement at first approximates the Doppler factor followed by balancing through the collected PN structure. The later step predicts the channel with the aid of sparse recovery greedy algorithm, look-ahead, and backtracking orthogonal matching pursuit (LABOMP). The LABOMP was applied to the chosen small IBI-free region to get better recovery and ignore the IBI effect. LABOMP is used as multistage estimation providing better signal recovery. The proposed CS-based schemes are applied in real field measurements and show better energy, spectral, and BER performance. Compared to convention TDS-OFDM schemes, the proposed one provides reliable underwater communication.

The paper is structured to discuss the detailed model of the system in Section II while Section III explains the technique for channel estimation applied to the underwater

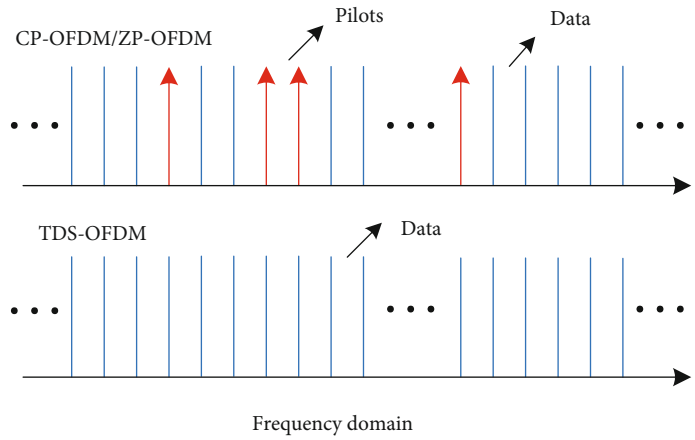

Figure 1: The frequency domain response of the OFDM standard signal structure.

acoustic channel based on compressive sensing. Section IV provides the simulation results followed by their validation through experimental results and discussion in Section V. Finally, the conclusive summary of the article is given in Section VI.

2. Model of the System

As we know, CP-OFDM, TDS-OFDM, and ZP-OFDM are the three different types of the OFDM system that are widely applicable in the technology of wireless communication [13, 31]. CP has been used as guard interval for CP-OFDM, ZP has been considered in ZP-OFDM as guard interval, and PN sequences are inserted as guard interval in TDS-OFDM. The comparative analysis of the structure of the signal, for the ZP-OFDM, TDS-OFDM, and CP-OFDM, in the frequency domain is shown in Figure 1 [23]. In comparison to the maximum delay of the time-varying multipath channel, the length of the guard interval (GI) must be larger so the information data block is not affected by ISI or IBI [3]. To evade the IBI issue in the multipath channel, the IBI-free region i^{th} transmitted OFDM block can be mathematically formulated as:

$$\boldsymbol{x}_i = [\boldsymbol{p}_i, \boldsymbol{d}_i]^T_{M+NX1}, \tag{1}$$

where $\boldsymbol{p}_i = \{p_{i,k}\}_{k=0}^{M-1}$, M is the PN sequence length, $\boldsymbol{d}_i = \{d_{i,k}\}_{k=0}^{N-1}$, k signifies the k^{th} constituent of the i^{th} block of the TDS-OFDM, and N specifies the length of the block for the OFDM information data.

3. Channel Estimation Based on CS for Underwater Communication

The interference in TDS-OFDM comprises several characteristics in a way that the perfect detection over multiple channels is difficult to achieve for the unknown OFDM data blocks. Figure 2 depicts this response behavior. Owing to the data block of the OFDM, it is a difficult task to anticipate and mitigate IBI completely in support of the perfectly employed channel estimation techniques. Furthermore, because of the large size of the data block for the OFDM, the computational complexity is increased while calculating IBI. The training sequence is exploited on the receiver end besides knowing the training sequences; therefore, the IBI can then be computed only after the successful and accurate achievement of channel estimation [3]. While estimating channels accurately and overlooking the effects of the data block for OFDM on the sequence of training, there will be a resulting unmanageable mutual interference. The small IBI-free region exists because of the margin design of the system within the training received and is also analyzed in some practical applications. The worst case for the CP-OFDM and TDS-OFDM is observed in the equivalent channel length and guard interval. To avoid such a scenario, it is better to increase the guard size and minimize the channel length to achieve perfect estimation while avoiding the IBI. Figure 3 shows the proposed transceiver model.

The perfect channel estimation results in the complete elimination of the interference induced mutually from the data block of the TDS-OFDM. The ZP-OFDM system and the TDS-OFDM scheme, after ignoring the PN sequence, depict the same results. The technique of the DPN-TDS-OFDM dealt with the problem of the mutual interference, in the conventional TDS-OFDM system, arising from the data block to the PN sequence. The perfect channel estimation while ignoring the IBI and duplication of the guard interval to get a PN sequence is achieved in the DPN-TDS-OFDM frame. Figure 2 depicts the results of the TDS-OFDM schemes for multipath channels. The IBI affected the received PN sequence due to the former data block of the OFDM in the multipath channel resulting in channel estimation. The channel estimation is obtained in the time domain for the TDS-OFDM system, and the PN sequence received can be expressed as:

$$\boldsymbol{r}_i = \boldsymbol{\varphi}_i \boldsymbol{h}_i + \boldsymbol{u}_i, \tag{2}$$

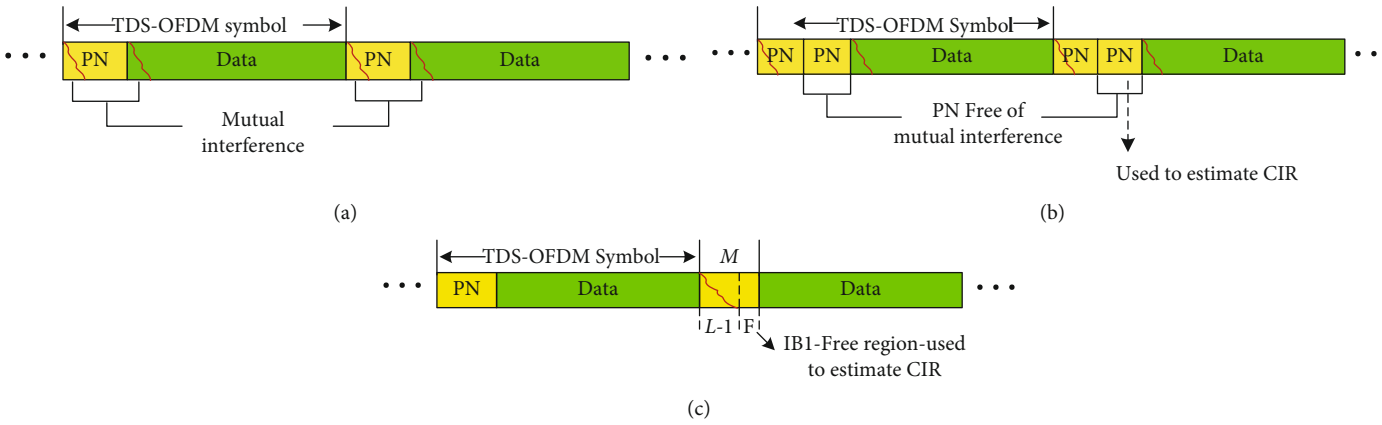

FIGURE 2: Received frame signal structure of different TDS-OFDM systems. (a) Conventional TDS-OFDM. (b) DPN-TDS-OFDM. (c) TDS-OFDM based on CS.

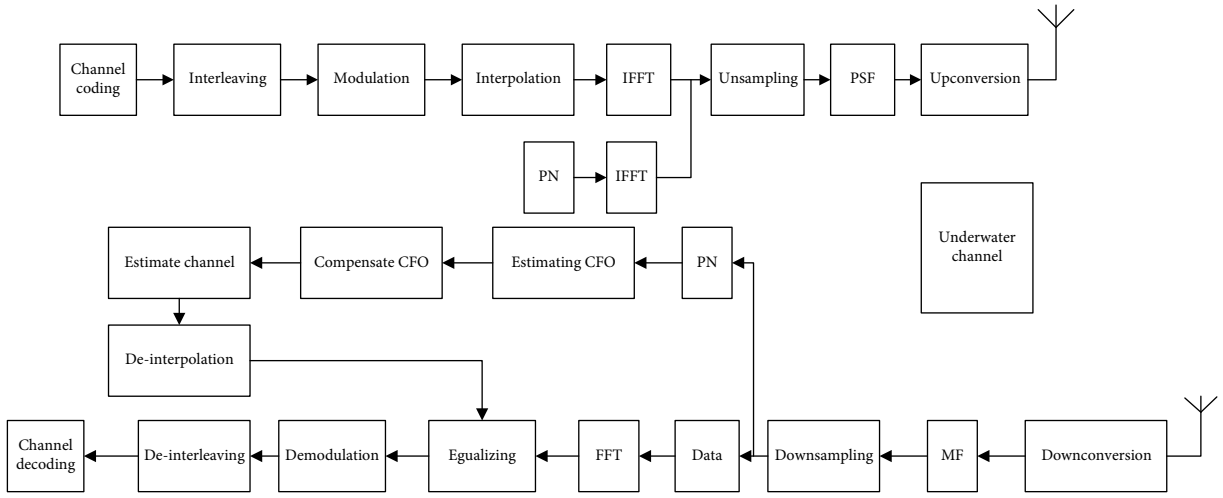

FIGURE 3: Block diagram of the transceiver proposed for the real underwater experiment.

where $\boldsymbol{u}_i$ signifies the AWGN noise having a mean value of zero and variance σ^2. $\boldsymbol{\varphi_i}$ can be mathematically represented as:

$$\boldsymbol{\varphi_i} = \begin{bmatrix} p_{i,0} & d_{i-1,N-1} & \cdots & d_{i-1,N-L+1} \\ p_{i,1} & p_{i,0} & \cdots & d_{i-1,N-L+2} \\ \vdots & \vdots & \ddots & \vdots \\ p_{i,L-1} & p_{i,L-2} & \cdots & p_{i,0} \\ p_{i,L} & p_{i,L-1} & \cdots & p_{i,1} \\ \vdots & \vdots & \ddots & \vdots \\ p_{i,M-1} & p_{i,M-2} & \cdots & p_{i,M-L} \end{bmatrix}_{MXL}. \quad (3)$$

The $i-1$th element shows the last transmitted block that interferes with the present symbol of the TDS-OFDM in eq. (3). It can be observed that the preceding samples, i.e., $M-L+1$, show no corrupted signals generating from the previous data blocks of the TDS-OFDM. Therefore, the CS theory utilizes the IBI-free region for the estimation of the channel. The observation matrix is introduced by extracting the preceding $F = M - L + 1$. A new sub-matrix is developed and is mathematically expressed as:

$$\boldsymbol{\Phi} = \begin{bmatrix} p_{i,L-1} & p_{i,L-2} & \cdots & p_{i,0} \\ p_{i,L} & p_{i,L-1} & \cdots & p_{i,1} \\ \vdots & \vdots & \ddots & \vdots \\ p_{i,M-1} & p_{i,M-2} & \cdots & p_{i,M-L} \end{bmatrix}_{FXL}. \quad (4)$$

The PN sequence is used to obtain the observation matrix F-X-L size. Eventually, the noise in IBI-free region corrupts the received signal and thus can be denoted as under:

$$\boldsymbol{y_i} = \boldsymbol{\Phi_i h_i} + \boldsymbol{u_i}. \quad (5)$$

3.1. Proposed Algorithm. The energy and spectrum in the UWA communication can be saved by minimizing the free IBI regions in TDS-OFDM. Thus, a small IBI-free region is

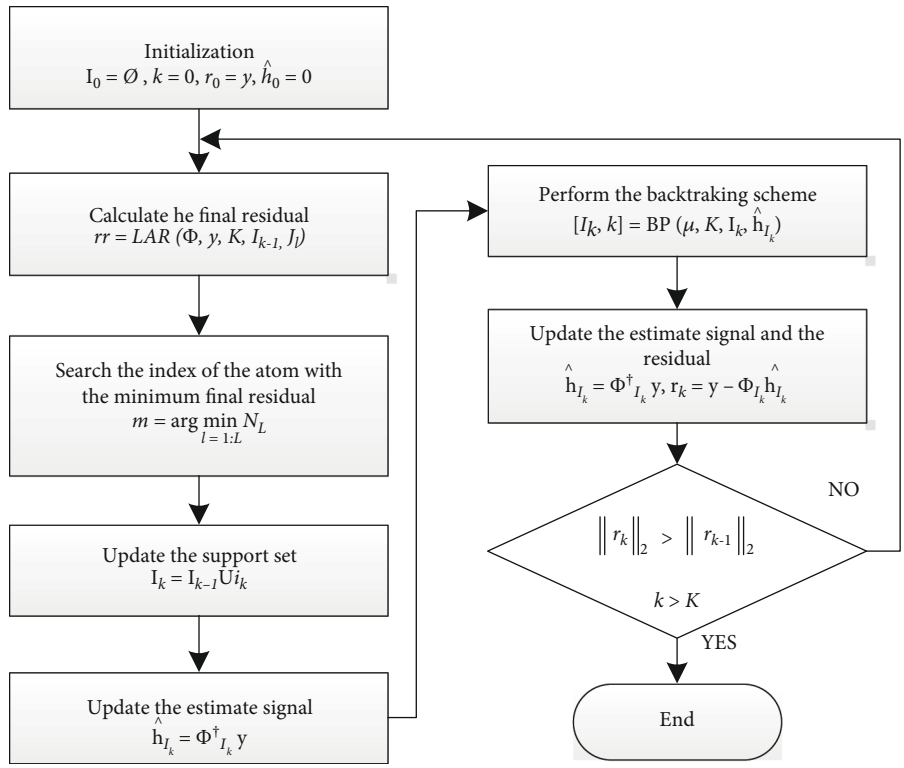

Figure 4: Flow chart of our proposed LABOMP algorithm for underwater acoustic channel estimation.

used and a LABOMP algorithm is proposed in this paper to address this issue. The backtracking pruning (BP) and look-ahead residue (LAR) functions are utilized in the LABOMP algorithm [3], by implementing the backtracking and look-ahead scheme, respectively. In the LABOMP algorithm flow chart depicted in Figure 4, the steps of the LAR function are presented in algorithm 1. In the first part, the potential l atoms are chosen that are more correlative with the residue of the last loop using a fixed look-ahead parameter l. In the second step, the support set is obtained by selecting the best one before predicting the effects of each potential atom. The residue and estimated signals are updated in the third step. Finally, the termination condition of the algorithm is evaluated by determining the current iteration status.

Functions 1 and 2 are defined by utilizing the flow chart of LABOMP in Figure 4. The second step of the LABOMP flow chart shows that K is the sparsity level and Function 1 is the look-ahead residual set, where $\boldsymbol{r} \in R^{FX1}$ and $\boldsymbol{\Phi} \in R^{FXL}$. The parameter $\boldsymbol{I}$ and i represent the set of intermediate support and optimal atom index in the current iteration, respectively. Hence, the given algorithmic function is used to find the output residual $\boldsymbol{rr} \in R^F$. Function 2 is the backtracking pruning and is shown in step 6 of the LABOMP flow chart, where K is the sparsity level and $\mu \in [0, 1]$ by considering that the $\hat{h}_{I_k}$ is the estimated signal passing LAR function and I_k is the present selected set of intermediate support. Thus, the backtracking k and the new index of atoms I_k are obtained by using the following algorithmic function. The total iterations are divided into two types by the backtracking scheme that comprises cascade backtracking and a dominant look-ahead convergence. The stage of the cascade backtracking is triggered by the preset constant threshold, i.e., $\lambda = \mu \cdot K$, that deletes the incorrect selected atoms in the last iteration. Moreover, the rule for adding atoms and signal structure has been associated with λ and the anticipated empirical value for LABOMP algorithm is $0.8K \sim 0.9K$. Algorithm 2 depicts the twofold idea of the BP function. In the first step, dominant look-ahead convergence provides the correct large coefficient atoms. The mismatched atoms that are selected in the previous iteration are not strictly orthogonal due to small coefficients. Therefore, to prune the maximum mismatching atoms, the scheme of backtracking utilizes the support set in the second step [3].

4. Simulation Results and Discussion

4.1. Spectral Efficiency. The mathematical formulation of spectral efficiency for OFDM systems has been presented in [23]:

$$\text{SpectralEfficiency} = \left(\frac{N_{\text{Data}}}{N_{\text{Data}} + P_{\text{Pilots}}} \times \frac{N_{\text{Frame}}}{N_{\text{Frame}} + M}\right) \times 100\%, \tag{6}$$

where N_{Data} denotes the data size (data subcarriers) and P_{Pilots} signifies the pilot sub-carriers, M shows the guard interval length, and N_{Frame} is the length of the frame (data subcarriers and pilots subcarriers). Figure 5 relates the spectral efficiency of our proposed method LABOMP with DPN-TDS-OFDM, TDS-OFDM, and conventional CP-OFDM.

Input: Sparsity K, $\boldsymbol{y} \in \mathbb{R}^{F\times 1}$, $\boldsymbol{\Phi} \in \mathbb{R}^{F\times L}$, newly selected index i, previous support set $\boldsymbol{I}$;
Initialization: The approximate coefficient $\widehat{\boldsymbol{h}}_{I_k} = \boldsymbol{\Phi}_{I_k}^{\dagger}\boldsymbol{y}$, residual $\boldsymbol{r}_k = \boldsymbol{y} - \boldsymbol{\Phi}_{I_k} \cdot \widehat{\boldsymbol{h}}_{I_k}$, the intermediate support set $\boldsymbol{I}_k = \boldsymbol{I}_k \cup i$, counter $k = |\boldsymbol{I}_k|$;
Repeat:
$k = k + +$;
$i_k = argmax_{i=1}^{N} \boldsymbol{\Phi}_i^T \boldsymbol{r}_{k-1}$, $i \notin \boldsymbol{I}_{k-1}$; matching the filter values
$\boldsymbol{I}_k = \boldsymbol{I}_k \cup i$; updating support set
$\widehat{\boldsymbol{h}}_{I_k} = \boldsymbol{\Phi}_{I_k}^{\dagger}\boldsymbol{y}$;
$\boldsymbol{r}_k = \boldsymbol{y} - \boldsymbol{\Phi}_{I_k} \cdot \widehat{\boldsymbol{h}}_{I_k}$;
Until $\|\boldsymbol{r}_{k-1}\|_2 < \|\boldsymbol{r}_k\|_2$ or $k > K$
Output: $\boldsymbol{r}_k = \boldsymbol{y} - \boldsymbol{\Phi}_{I_k}\boldsymbol{\Phi}_{I_k}^{\dagger}\boldsymbol{y}$;

Algorithm 1: LAR algorithm

Input: K, $\widehat{\boldsymbol{h}}_{I_k}$, μ, $\boldsymbol{I}_k$;
Initialization: $\lambda = \mu K$;
while $k \geq \lambda$ & $k\%2 = 1$
$[v, pp] = argmin|\widehat{\boldsymbol{h}}_{I_k}|$;
$I_k = \boldsymbol{I}_k \setminus pp$ the minimum value of $\widehat{\boldsymbol{h}}_{I_k}$ to eliminate
end while
Output: I_k, pp;

Algorithm 2: BP algorithm

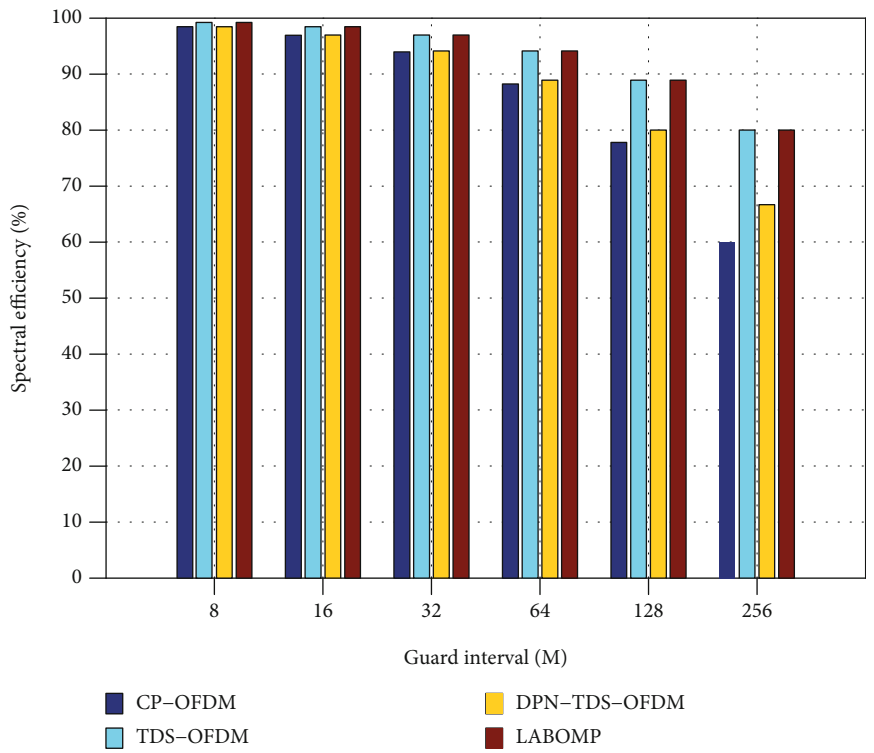

Figure 5: Spectral efficiency comparison of CP-OFDM, TDS-OFDM, DPN-TDS-OFDM, and proposed LABOMP-TDS-OFDM.

Despite the consistent and fast synchronization, TDS-OFDM, due to the removal of pilots, shows more spectral efficiency in comparison to CP-OFDM systems. Here, the consequence of these advantages is more critical and crucial to revoke the iterative interfering because of the mutual interference in between the PN sequence (guard interval) and the

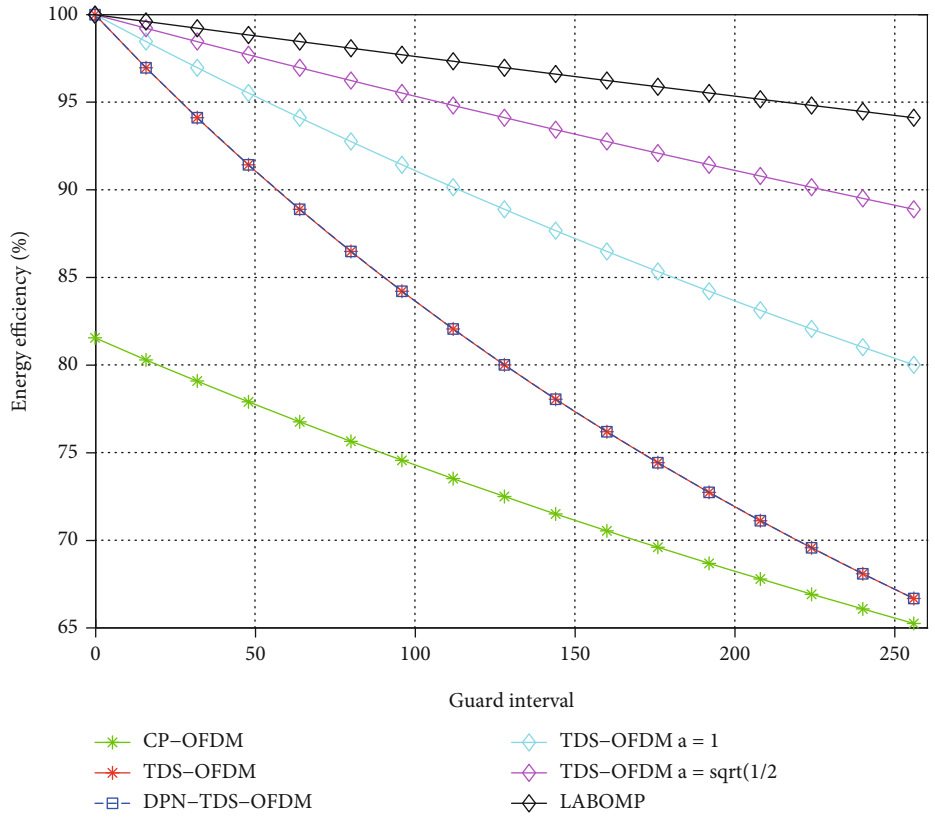

Figure 6: Energy efficiency comparison of CP-OFDM, conventional TDS-OFDM, DPN-TDS-OFDM, TDS-OFDM a=1, TDS-OFDM a= sqrt (1/2), and proposed LABOMP-TDS-OFDM.

Table 1: System specifications of parameters.

Parameters	Values
PN sequence (M)	255
Data block (N)	1024
Free-region length in channel (F)	75
Channel size (L)	255
Bandwidth	6*KHz*
Carrier frequency	20*KHz*
Sampling frequency	96*KHz*
Central frequency	30*KHz*
Modulation	QPSK
Data rate	11.99 kbits/sec
OFDM symbol duration	170.67 msec
CFO	0.2

data block of OFDM. Double the PN sequences in DPN-TDS-OFDM cancel out the interferences but the spectral efficiency was highly affected. There is no alteration required in the structure of the TDS-OFDM system while using the CS concept into TDS-OFDM, so the spectral efficiency has been improved concerning BER and MSE with high performance. Figure 5 depicts the spectral efficiency comparison of LABOMP-TDS-OFDM with conventional TDS-OFDM, conventional CP-OFDM, and DPN-TDS-OFDM.

4.2. Energy Efficiency. The energy efficiency for OFDM systems has been formulated in [23]:

$$\text{EnergyEfficiency} = \left(\frac{N_{\text{Data}}}{N_{\text{Data}} + b^2 P_{\text{Pilots}}} \times \frac{N_{\text{Frame}}}{N_{\text{Frame}} + a^2 M}\right) \times 100\% \quad (7)$$

where a and b signify the amplitude factor imposed on the guard interval and the amplitude factor imposed on the pilots in the time and frequency domain, respectively. The pilot's amplitudes have been increased for CP-OFDM requirement which increases the receiver channel estimation performance such as $b = 4/3$ has been identified by the digital video broadcasting second generation terrestrial (DVB-T2) standard [23, 32]. Similarly, to guarantee the reliable channel estimation in TDS-OFDM, the amplitude of PN sequences has been increased; DTMB standard indicated the value of $a = \sqrt{2}$ [23, 33]. Alternatively, channel estimation performance of CS-based proposed LABOMP-TDS-OFDM has been improved with IBI-free region. IBI-free region has been employed in the LABOMP-TDS-OFDM so the guard interval does not require a high power; hence, the used PN training sequence amplitude is designated as $a = 0.5$. Figure 6 depicts the energy efficiency performance of TDS-OFDM, DPN-TDS-OFDM, CP-OFDM, and LABOMP-TDS-OFDM CS-based IBI-free region. In

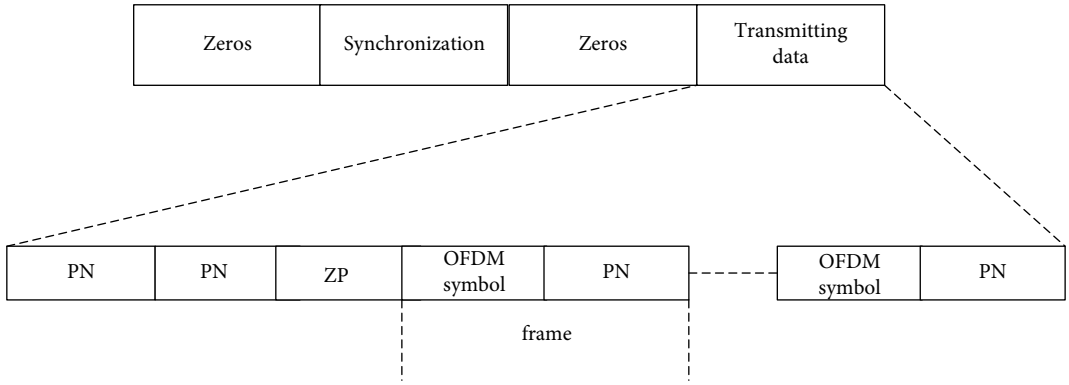

Figure 7: Frame structure of the transmitting signal.

Table 2: BER of OFDM received symbols at short distance.

Symbols	DPN	OMP	CoSaMP	LABOMP
1	0.0045	0.0032	0.0032	0.0018
2	0.0073	0.0053	0.0050	0.0042
3	0.0117	0.0086	0.0073	0.00671
4	0.0081	0.0053	0.0050	0.0039
5	0.0092	0.0072	0.0061	0.0048

Table 3: BER of OFDM received symbols with different distances.

Symbols	DPN	OMP	CoSaMP	LABOMP
1 m	0	0	0	0
10 m	0.0033	0.0019	0.0012	0.0008
30 m	0.0107	0.0062	0.0050	0.0031
100 m	0.0866	0.0583	0.0466	0.0311
1 km	0.0988	0.0662	0.0574	0.0446

CP-OFDM, the 4K mode of the DVB-T2 is used that result in the pilot occupation ratio of 11.29% [32]. The standard amplitude factor selected for DPN-TDS-OFDM and DTMB is 1 and $\sqrt{2}$, respectively [25].

4.3. Computational Complexity. We have noted from the proposed method that its performance mainly depends upon two parameters, present constant threshold λ and look-ahead parameter l. The better performance has been attained by increasing the value of l but it has a trade-off with computational complexity. Moreover, the performance can be not significantly improved with a small value of λ. The fact is that in the initial many iterations, atoms have been chosen with the larger value of coefficients, though the early matching backtracking has been suppressed. If the value of $l = 1$ and $\lambda = K$, LABOMP will behave like OMP. The complexity of LABOMP has been analyzed. It is known that multiplication operation is slower than summation so multiplication is mainly reported. The standard multiplication requires for matching filter FL while for estimating the spares channel requires $O(SF)$ multiplication by using least square (LS). The total iterations performed by LABOMP is $2S - \lambda + 1$. LABOMP computational complexity is $O(lS^2[1 + (S - \lambda)^2/S^2](SF + FL))$. In LAR, the LS estimator and matching filter multiplication cost are $O(lS^2[1 + (S - \lambda)^2/S^2])$ and total backtracking LS estimation cost is $(S - \lambda + 1)$.

The overall computational complexity of CoSaMP containing iterations equal to the sparsity level S is $O(4FS^3 + 8S^4)$ [34], and OMP is $O(FLS)$. In the conventional TDS-OFDM and DPN-OFDM, the channel is estimated based on the good features of the training sequence without interference cancelation. In these schemes, the received PN sequence directly correlated with the local PN sequence to generate the channel impulse response by efficiently implementing M-point fast Fourier transform; hence, these schemes have $\mathcal{O}((M/2)\log_2 M)$ [21, 22, 35].

5. Experimental Results and Discussion

The real data experiment was first conducted in the water tank for testing. Furthermore, it was also conducted in the sea at Wuyuan sea area Xiamen, China. The experimental field depth in the tank is almost 1 m. We have transmitted the signal from one transducer at the water depth of 1 m, and the signal was received by another transducer at the depth of 1 m also. The experimental depth of both transmitter and receiver was almost 3 m in the sea, and the distances between transmitter and receivers were almost 1 m, 10 m, 30 m, 100 m, and 1 Km, respectively. The sea experiment was done on different distances.

In the TDS-OFDM system, the total number of carriers only contained data subcarriers and there is no pilot subcarrier. The channel is estimated by guard interval (PN sequences). The parameters' specification of real sea testing is shown in Table 1. The transmitting frame structure of OFDM data is shown in Figure 7. The frame structure includes zeros vector with length of 120, linear frequency modulation (LFM) pulse vector has the 4096 sizes, after LFM there are zeros that has the length of 12000, and in the end is the transmitting data (OFDM symbols). There are five symbols, each symbol has five frames, and every frame size is 2560. For synchronization, auto-correlation

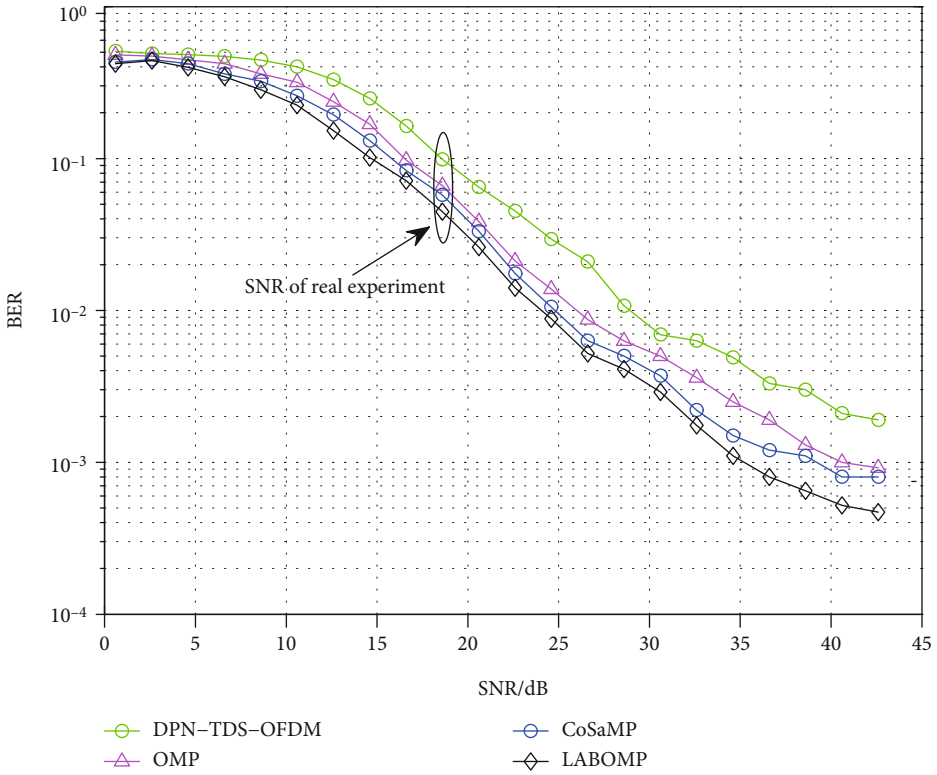

Figure 8: BER comparison of semi experiment DPN-TDS-OFDM, OMP, CoSaMP, and LABOMP.

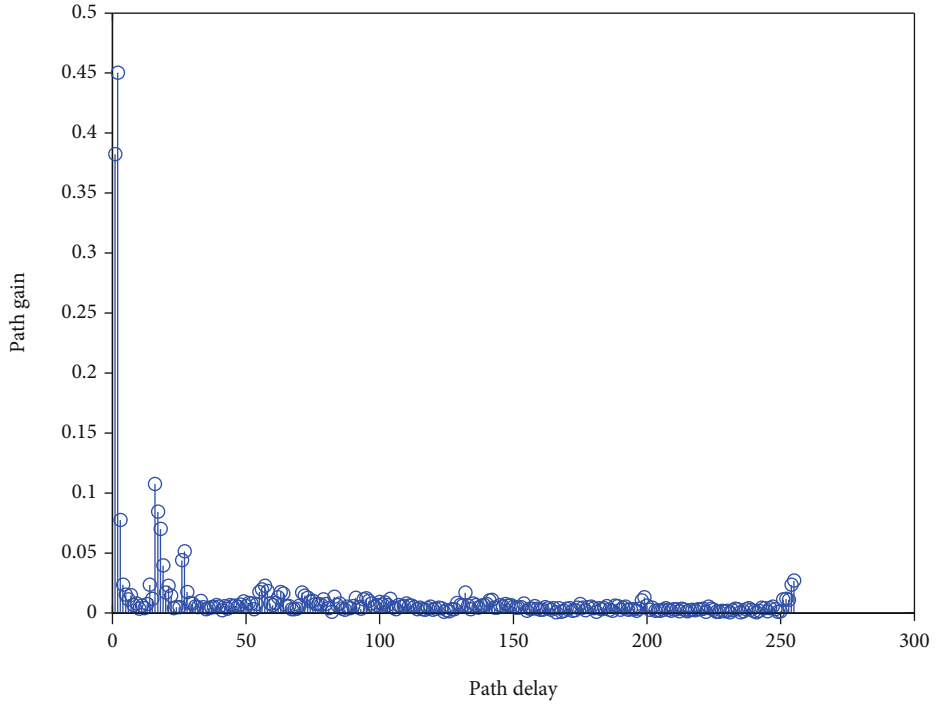

Figure 9: Underwater estimated CIR by known PN sequence.

method has been utilized to find the starting point of the signal for exact data recovery after channel estimation.

The performance evaluation of the TDS-OFDM system in the UWA channel has compared the DPN-TDS-OFDM and compressed sensing-based methods, namely, OMP, CoSaMP, and LABOMP. First, the channel is estimated by all these methods in the time domain. After the channel estimation, the results are for data demodulation in the form

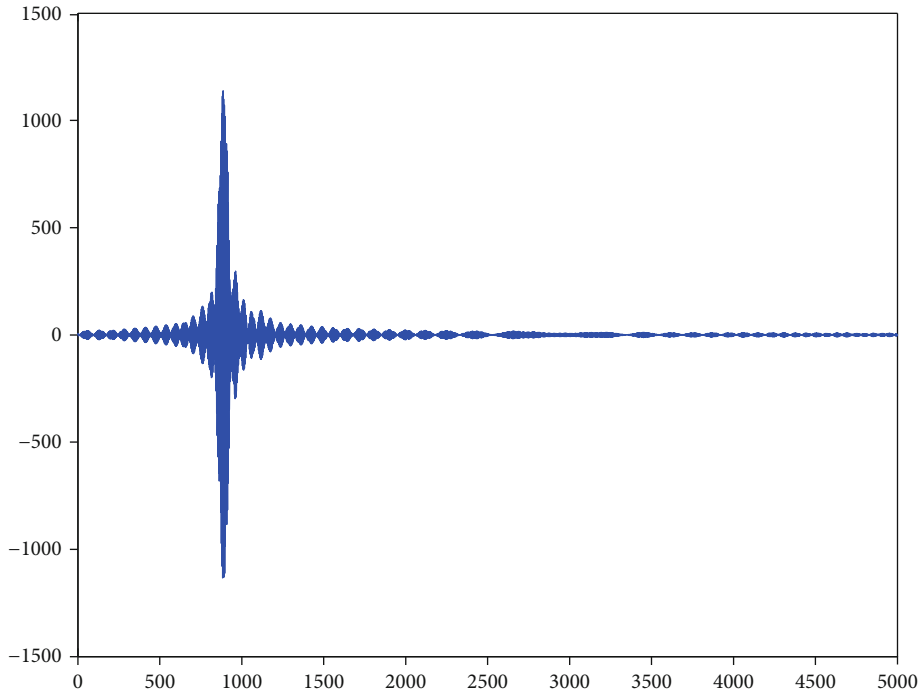

Figure 10: LFM-based auto-correlation.

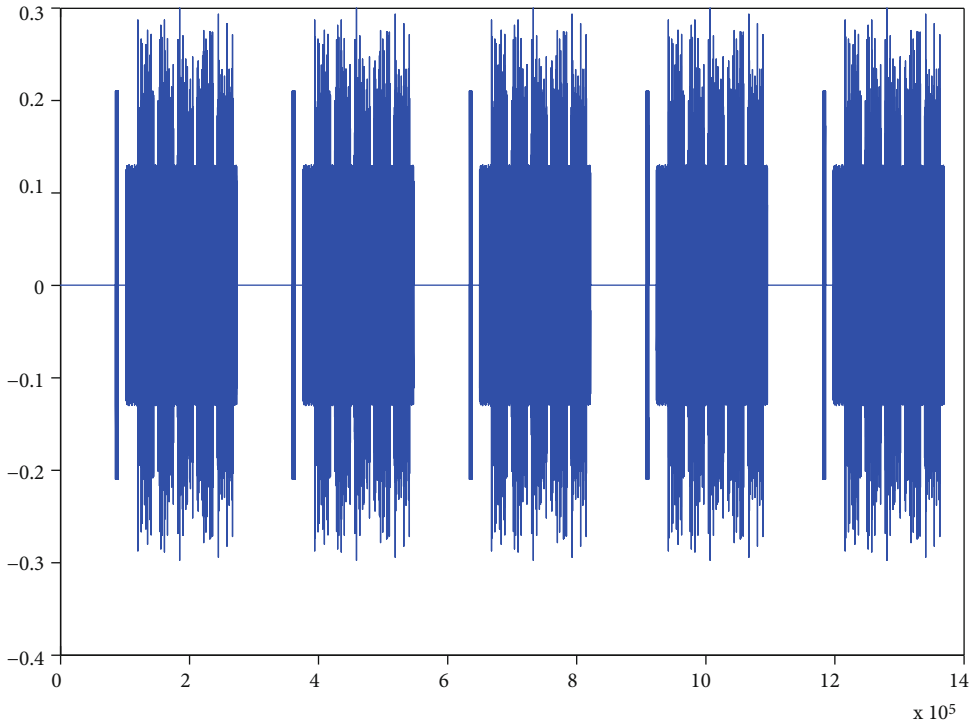

Figure 11: OFDM transmitting signal before sending over the underwater acoustic channel.

MMSE equalizer to ease the channel estimation method performance evaluation. In last, data is detected in the frequency domain. The LABOMP is for the first time proposed for underwater TDS-OFDM system which outperforms in comparison of DPN, OMP, and CoSaMP. The different channel estimation method's performance has been analyzed using PN sequences. In DPN-TDS-OFDM channel, it is estimated by using two repeated PN sequences; for OMP, CoSaMP, and LABOMP channel, estimation is done by using IBI-free region in the received PN sequence.

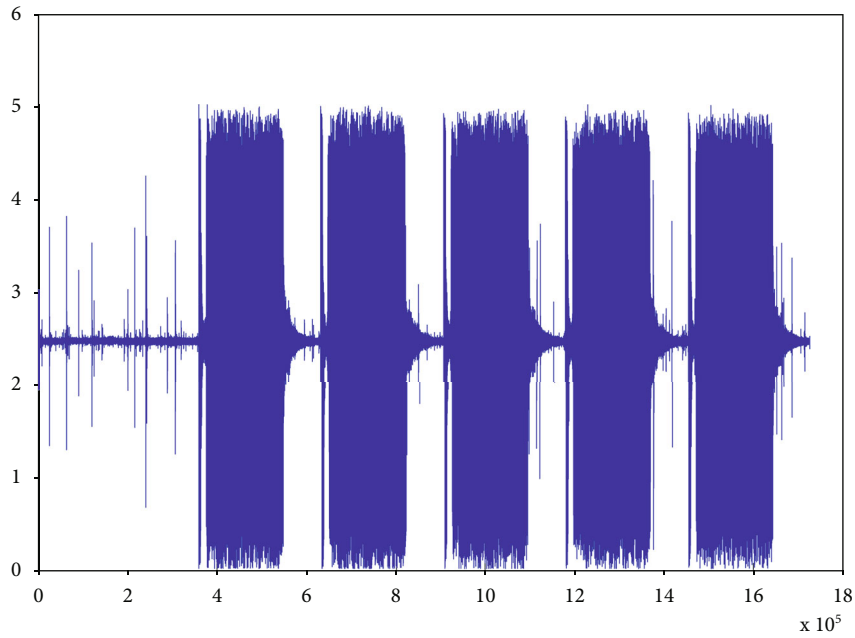

Figure 12: OFDM received signal through the underwater acoustic channel.

Figure 13: Field area of a real experiment.

Table 2 shows the BER of five received OFDM data symbols. These results of BER have been attained at a short distance of almost 10 m between transmitter and receiver. It is clearly shown that all techniques give better BER performance at a short distance. All CS-based methods outperform DPN-TDS-OFDM in terms of BER, but LABOMP gives better performance than OMP and CoSaMP. Table 3 depicts the BER performance of DPN-TDS-OFDM, OMP, CoSaMP, and LABOMP at different distances as 1 m, 10 m, 30 m, 100 m, and 1 Km. At a distance of 1.5 m, all methods give outstanding performance in terms of BER. As the distance is going to increase, the BER is affected. Our proposed CS-

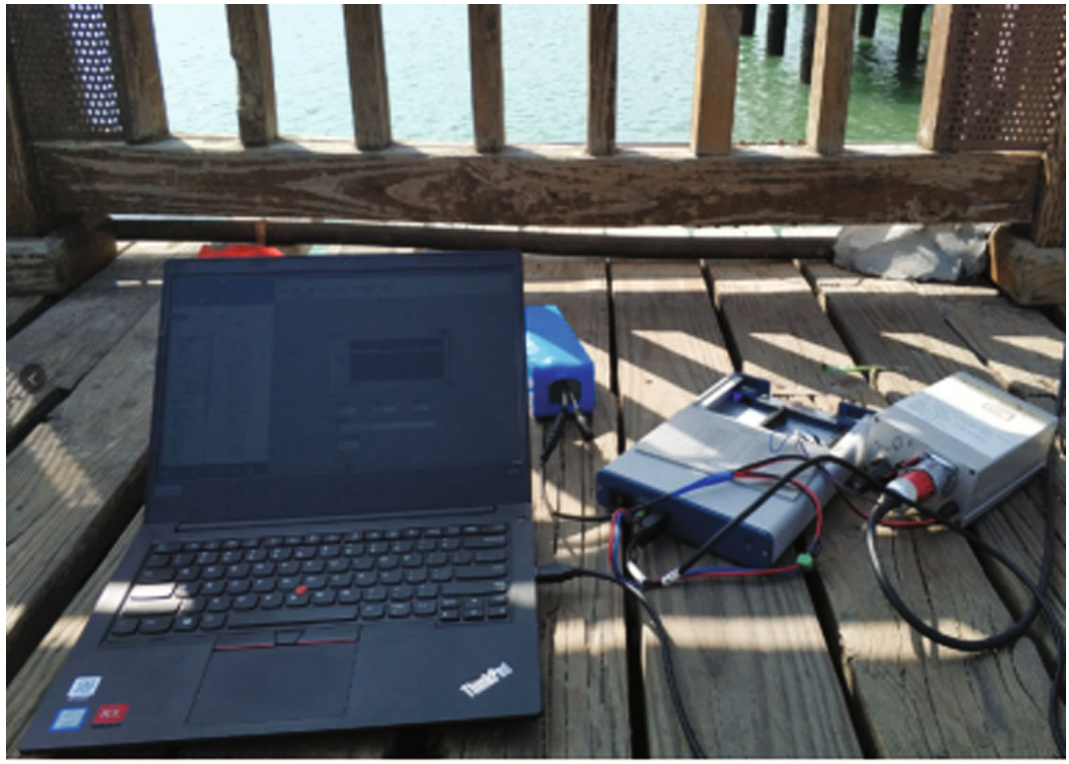

Figure 14: Instruments used for real sea experiment.

based greedy algorithm, namely, LABOMP, gives better performance in terms of BER as compared to other methods including DPN-TDS-OFDM, OMP, and CoSaMP.

The BER performance of the semi experiment with DPN-TDS-OFDM, OMP, CoSaMP, and LABOMP is shown in Figure 8. Thanks to the sparse nature of the UWA channel, it is seen that greedy algorithms outperform DPN-TDS-OFDM in terms of BER with different SNR gains. But, luckily the LABOMP algorithm also gives better performance in terms of BER compared to OMP and CoSaMP. The SNR of the channel is 18.6 dB. Figure 9 depicts the CIR of the OFDM data symbol which is estimated by a known PN sequence. As we say, the UWA channel is multipath and sparse, so it is seen in Figure 9.

Figure 10, Figure 11, and Figure 12 show the auto-correlation, OFDM transmitted signal, and received signal from the UWA channel, respectively. In Figure 10, LFM has been used to find the synchronization point. As we know auto-correlation gives the highest point at the beginning of the signal, so in this way, we get the starting point of the signal at receiving side. It is seen from Figure 12, that signal is affected by UWA channel and noise also, even there is a delay in received signal as compared to transmitted signal as seen in Figure 11. In real-time, the receiver has to wait for the information which will be sent by the transmitter.

Figure 13 depicts the map of the allocation where we have tasted underwater real-time experiments. The experiment was tested at different distances from 1 m to almost 1 Km. The black straight line in Figure 13 shows the long-distance experiment is 967 m which is almost equal to 1 Km. Figure 14 illustrates the hardware system which has been used for the sea experiment. The hardware system contains a laptop, battery, power amplifier, and analog to digital (A/D) converter. For a real sea experiment, the transmitting data has been saved in a MATLAB file (.m). After that, the data format has been converted to .bin format. That.bin file has been transmitted wireless from one computer to another using LABVIEW on both sides.

6. Conclusion

In this paper, algorithms for the UWA TDS-OFDM have been proposed based on CS to curtail the IBI for sparse channel estimation between PN training sequence and data frames. The IBI-free region in PN sequences plays a vital role; the channel has been properly reconstructed by CS-based techniques to attain higher EE and SE. PN sequence has been utilized to estimate and compensate the Doppler shift. In the real sea testing, experimental results show that the performance of the CS-based algorithms is much better than the DPN-TDS-OFDM and TDS-OFDM. A relevant comparison is performed among LABOMOP, CoSaMP, and OMP to observe the effectiveness of each CS-based algorithm. It is evident from the simulation and experimental results that the LABOMOP outperforms the conventional CS algorithms such as CoSaMP and OMP. Furthermore, the proposed CS-based methods achieved better spectral SE, EE, and substantial BER improvement for TDS-OFDM in comparison with conventional systems.

Data Availability

The data used to support the findings of this study are available from the corresponding author upon request.

Conflicts of Interest

The authors declare no conflict of interest.

Acknowledgments

This paper is based upon work supported by Science, Technology & Innovation Funding Authority (STDF) under grant number 46143.

References

[1] H. Esmaiel, Z. A. H. Qasem, H. Sun, J. Wang, and N. U. Rehman Junejo, "Underwater image transmission using spatial modulation unequal error protection for internet of underwater things," *Sensors*, vol. 19, no. 23, pp. 5271–5284, 2019.

[2] X. Ma, F. Yang, S. Liu, and J. Song, "Channel estimation for wideband underwater visible light communication: a compressive sensing perspective," *Optics Express*, vol. 26, no. 1, pp. 311–321, 2018.

[3] N. U. R. Junejo, H. Esmaiel, M. Zhou, H. Sun, J. Qi, and J. Wang, "Sparse channel estimation of underwater TDS-OFDM system using look-ahead backtracking orthogonal matching pursuit," *IEEE Access*, vol. 6, pp. 74389–74399, 2018.

[4] M. Mostafa, H. Esmaiel, and E. M. Mohamed, "A comparative study on underwater communications for enabling C/U plane splitting based hybrid UWSNs," in *2018 IEEE Wireless Communications and Networking Conference*, pp. 1–6, Barcelona, Spain, April 2018.

[5] I. Iglesias, A. Song, J. Garcia-Frias, M. Badiey, and G. R. Arce, "Image transmission over the underwater acoustic channel via compressive sensing," in *2011 45th Annual Conference on Information Sciences and Systems*, pp. 1–6, Baltimore, MD, USA, March 2011.

[6] J. Li and Y. V. Zakharov, "Efficient use of space-time clustering for underwater acoustic communications," *IEEE Journal of Oceanic Engineering*, vol. 43, no. 1, pp. 173–183, 2018.

[7] Y. V. Zakharov and A. K. Morozov, "OFDM transmission without guard interval in fast-varying underwater acoustic channels," *IEEE Journal of Oceanic Engineering*, vol. 40, no. 1, pp. 144–158, 2015.

[8] C. R. Berger, Z. Wang, J. Huang, and S. Zhou, "Application of compressive sensing to sparse channel estimation," *IEEE Communications Magazine*, vol. 48, no. 11, pp. 164–174, 2010.

[9] S. Kaddouri, P.-P. J. Beaujean, and P.-J. Bouvet, "High-frequency acoustic estimation of time-varying underwater sparse channels using multiple sources and receivers operated simultaneously," *IEEE Access*, vol. 6, pp. 10569–10580, 2018.

[10] Z. Yang and Y. R. Zheng, "Iterative channel estimation and turbo equalization for multiple-input multiple-output underwater acoustic communications," *IEEE Journal of Oceanic Engineering*, vol. 41, no. 1, pp. 232–242, 2016.

[11] X. Ma, F. Yang, S. Liu, W. Ding, and J. Song, "Structured compressive sensing-based channel estimation for time frequency training OFDM systems over doubly selective channel," *IEEE Wireless Communications Letters*, vol. 6, no. 2, pp. 266–269, 2017.

[12] L. Dai, Z. Wang, and Z. Yang, "Time-frequency training OFDM with high spectral efficiency and reliable performance in high speed environments," *IEEE Journal on Selected Areas in Communications*, vol. 30, no. 4, pp. 695–707, 2012.

[13] H. Esmaiel and D. Jiang, "Zero-pseudorandom noise training OFDM," *Electronics Letters*, vol. 50, no. 9, pp. 650–652, 2014.

[14] B. Muquet, Z. Wang, G. B. Giannakis, M. De Courville, and P. Duhamel, "Cyclic prefixing or zero padding for wireless multicarrier transmissions," *IEEE Transactions on Communications*, vol. 50, no. 12, pp. 2136–2148, 2002.

[15] J. Wu, Y. Chen, X. Zeng, and H. Min, "Robust timing and frequency synchronization scheme for DTMB system," *IEEE Transactions on Consumer Electronics*, vol. 53, no. 4, pp. 1348–1352, 2007.

[16] W. Ding, F. Yang, W. Dai, and J. Song, "Time–frequency joint sparse channel estimation for MIMO-OFDM systems," *IEEE Communications Letters*, vol. 19, no. 1, pp. 58–61, 2015.

[17] E. Başar, Ü. Aygölü, E. Panayırcı, and H. V. Poor, "Orthogonal frequency division multiplexing with index modulation," *IEEE Transactions on Signal Processing*, vol. 61, no. 22, pp. 5536–5549, 2013.

[18] M. Wen, B. Ye, E. Basar, Q. Li, and F. Ji, "Enhanced orthogonal frequency division multiplexing with index modulation," *IEEE Transactions on Wireless Communications*, vol. 16, no. 7, pp. 4786–4801, 2017.

[19] J. Li, S. Dang, M. Wen, X.-Q. Jiang, Y. Peng, and H. Hai, "Layered orthogonal frequency division multiplexing with index modulation," *IEEE Systems Journal*, vol. 13, no. 4, pp. 3793–3802, 2019.

[20] M. Wen, X. Cheng, L. Yang, Y. Li, X. Cheng, and F. Ji, "Index modulated OFDM for underwater acoustic communications," *IEEE Communications Magazine*, vol. 54, no. 5, pp. 132–137, 2016.

[21] J. Wang, Z.-X. Yang, C.-Y. Pan, J. Song, and L. Yang, "Iterative padding subtraction of the PN sequence for the TDS-OFDM over broadcast channels," *IEEE Transactions on Consumer Electronics*, vol. 51, no. 4, pp. 1148–1152, 2005.

[22] M. Liu, M. Crussiere, and J.-F. Hélard, "A novel data-aided channel estimation with reduced complexity for TDS-OFDM systems," *IEEE Transactions on Broadcasting*, vol. 58, no. 2, pp. 247–260, 2012.

[23] L. Dai, J. Wang, Z. Wang, P. Tsiaflakis, and M. Moonen, "Spectrum-and energy-efficient OFDM based on simultaneous multi-channel reconstruction," *IEEE Transactions on Signal Processing*, vol. 61, no. 23, pp. 6047–6059, 2013.

[24] M. Huemer, C. Hofbauer, and J. B. Huber, "Non-systematic complex number RS coded OFDM by unique word prefix," *IEEE Transactions on Signal Processing*, vol. 60, no. 1, pp. 285–299, 2012.

[25] J. Fu, J. Wang, J. Song, C.-Y. Pan, and Z.-X. Yang, "A simplified equalization method for dual PN-sequence padding TDS-OFDM systems," *IEEE Transactions on Broadcasting*, vol. 54, no. 4, pp. 825–830, 2008.

[26] L. Dai, Z. Wang, and Z. Yang, "Next-generation digital television terrestrial broadcasting systems: key technologies and research trends," *IEEE Communications Magazine*, vol. 50, no. 6, pp. 150–158, 2012.

[27] L. Dai, Z. Wang, and Z. Yang, "Spectrally efficient time-frequency training OFDM for mobile large-scale MIMO systems," *IEEE Journal on Selected Areas in Communications*, vol. 31, no. 2, pp. 251–263, 2013.

[28] W. Ding, F. Yang, C. Pan, L. Dai, and J. Song, "Compressive sensing based channel estimation for OFDM systems under long delay channels," *IEEE Transactions on Broadcasting*, vol. 60, no. 2, pp. 313–321, 2014.

[29] X. Ma, F. Yang, S. Liu, J. Song, and Z. Han, "Design and optimization on training sequence for mmWave communications: a new approach for sparse channel estimation in massive MIMO," *IEEE Journal on Selected Areas in Communications*, vol. 35, no. 7, pp. 1486–1497, 2017.

[30] X. Ma, F. Yang, W. Ding, and J. Song, "Novel approach to design time-domain training sequence for accurate sparse channel estimation," *IEEE Transactions on Broadcasting*, vol. 62, no. 3, pp. 512–520, 2016.

[31] H. Esmaiel and D. Jiang, "Spectrum and energy efficient OFDM multicarrier modulation for an underwater acoustic channel," *Wireless Personal Communications*, vol. 96, no. 1, pp. 1577–1593, 2017.

[32] E. Etsi, "Digital video broadcasting," *Frame Structure Channel Coding and Modulation for a Second Generation Digital Terrestrial Television Broadcasting System*, vol. 1, 2012.

[33] B. T. Series, "Error-correction, data framing, modulation and emission methods for digital terrestrial television broadcasting," *International Telecommunication Union*, vol. 2011, 2011.

[34] L. Dai, Z. Wang, and Z. Yang, "Compressive sensing based timing domain synchronous OFDM transmission for vehicular communication," *IEEE Journal on Selected Areas in Communications*, vol. 31, no. 9, pp. 460–469, 2013.

[35] Z. Yang, X. Wang, Z. Wang, J. Wang, and J. Wang, "Improved channel estimation for TDS-OFDM based on flexible frequency-binary padding," *IEEE Transactions on Broadcasting*, vol. 56, no. 3, pp. 418–424, 2010.